

We are IntechOpen, the world's leading publisher of Open Access books Built by scientists, for scientists

6,900

Open access books available

186,000

International authors and editors

200M

Downloads

Our authors are among the

154

Countries delivered to

TOP 1%

most cited scientists

12.2%

Contributors from top 500 universities



WEB OF SCIENCE™

Selection of our books indexed in the Book Citation Index
in Web of Science™ Core Collection (BKCI)

Interested in publishing with us?
Contact book.department@intechopen.com

Numbers displayed above are based on latest data collected.
For more information visit www.intechopen.com



Elasto-Hydrodynamics of Quasicrystals and Its Applications

Tian You Fan¹ and Zhi Yi Tang²

¹Department of Physics, Beijing Institute of Technology, Beijing

²Southwest Jiaotong University Hope College, Nanchong, Sichuan
China

1. Introduction

Quasicrystal as a new structure of solids as well as a new material, has been studied over twenty five years. The elasticity and defects play a central role in field of mechanical behaviour of the material, see e.g. Fan [1]. Different from crystals and conventional engineering materials, quasicrystals have two different displacement fields: phonon field $u(u_1, u_2, u_3)$ and phason field $w(w_1, w_2, w_3)$, which is a new degree of freedom to condensed matter physics as well as continuum mechanics, this leads to two strain tensors such as

$$\varepsilon_{ij} = \frac{1}{2} \left(\frac{\partial u_i}{\partial x_j} + \frac{\partial u_j}{\partial x_i} \right), w_{ij} = \frac{\partial w_i}{\partial x_j} \quad (1)$$

We call the first of equation (1) as phonon strain tensor, the second as phason strain tensor, respectively. The corresponding stress tensor is σ_{ij} and H_{ij} .

The constitutive law is the so-called generalized Hooke's law as follows

$$\begin{aligned} \sigma_{ij} &= C_{ijkl} \varepsilon_{kl} + R_{ijkl} w_{kl} \\ H_{ij} &= K_{ijkl} w_{kl} + R_{kl ij} \varepsilon_{kl} \end{aligned} \quad (2)$$

in which C_{ijkl} denotes the phonon elastic tensor, K_{ijkl} the phason one, and R_{ijkl} the phonon-phason coupling one, respectively. It is evident that the appearance of the new degree freedom yields a great challenge to the continuum mechanics.

In the dynamic process of quasicrystals problem presents further complexity. According to the point of view of Lubensky et al. [2,3], phonon represents wave propagation, while phason represents diffusion in the dynamic process. Following the argument of Lubensky et al., Rochal and Lorman [4] and Fan [1,5] put forward the equations of motion of quasicrystals as follows

$$\rho \frac{\partial^2 u_i}{\partial t^2} = \frac{\partial \sigma_{ij}}{\partial x_j} \quad (3)$$

$$\kappa \frac{\partial w_i}{\partial t} = \frac{\partial H_{ij}}{\partial x_j} \quad (4)$$

Equation (3) is the equation of motion of conventional elastodynamics, and equation (4) is the linearized equation of hydrodynamics of Lubensky et al., so equations (3), (4) are elasto-hydrodynamic equations of quasicrystals.

The equations (1)-(4) are the basis of dynamic analysis of quasicrystalline material.

2. The elasto-hydrodynamics of two-dimensional decagonal quasicrystals and application to dynamic fracture

2.1 Statement of formulation and sample problem

Among over 200 quasicrystals observed to date, there are over 70 two-dimensional decagonal quasicrystals, so this kind of solid phases play an important role in the material. For simplicity, here only point group 10mm two-dimensional decagonal quasicrystals will be considered. We denote the periodic direction as the z axis and the quasiperiodic plane as the $x-y$ plane. Assume that a Griffith crack in the solid along the periodic direction, i.e., the z axis. It is obvious that elastic field induced by a uniform tensile stress at upper and lower surfaces of the specimen is independent of z , so $\partial(\)/\partial z = 0$. In this case, the stress-strain relations are reduced to

$$\begin{aligned} \sigma_{xx} &= L(\varepsilon_{xx} + \varepsilon_{yy}) + 2M\varepsilon_{xx} + R(w_{xx} + w_{yy}) \\ \sigma_{yy} &= L(\varepsilon_{xx} + \varepsilon_{yy}) + 2M\varepsilon_{yy} - R(w_{xx} + w_{yy}) \\ \sigma_{xy} &= \sigma_{yx} = 2M\varepsilon_{xy} + R(w_{yx} - w_{xy}) \\ H_{xx} &= K_1 w_{xx} + K_2 w_{yy} + R(\varepsilon_{xx} - \varepsilon_{yy}) \\ H_{yy} &= K_1 w_{yy} + K_2 w_{xx} + R(\varepsilon_{xx} - \varepsilon_{yy}) \\ H_{xy} &= K_1 w_{xy} - K_2 w_{yx} - 2R\varepsilon_{xy} \\ H_{yx} &= K_1 w_{yx} - K_2 w_{xy} + 2R\varepsilon_{xy} \end{aligned} \quad (5)$$

where $L = C_{12}$, $M = (C_{11} - C_{12})/2$ are the phonon elastic constants, K_1 and K_2 are the phason elastic constants, R phason-phason coupling elastic constant, respectively.

Substituting equations (5) into equations (3), (4) we obtain the equations of motion of decagonal quasicrystals as following:

$$\begin{aligned} \frac{\partial^2 u_x}{\partial t^2} &= c_1^2 \frac{\partial^2 u_x}{\partial x^2} + (c_1^2 - c_2^2) \frac{\partial^2 u_y}{\partial x \partial y} + c_2^2 \frac{\partial^2 u_x}{\partial y^2} + c_3^2 \left(\frac{\partial^2 w_x}{\partial x^2} + 2 \frac{\partial^2 w_y}{\partial x \partial y} - \frac{\partial^2 w_x}{\partial y^2} \right) \\ \frac{\partial^2 u_y}{\partial t^2} &= c_2^2 \frac{\partial^2 u_y}{\partial x^2} + (c_1^2 - c_2^2) \frac{\partial^2 u_x}{\partial x \partial y} + c_1^2 \frac{\partial^2 u_y}{\partial y^2} + c_3^2 \left(\frac{\partial^2 w_y}{\partial x^2} - 2 \frac{\partial^2 w_x}{\partial x \partial y} - \frac{\partial^2 w_y}{\partial y^2} \right) \\ \frac{\partial w_x}{\partial t} &= d_1^2 \left(\frac{\partial^2 w_x}{\partial x^2} + \frac{\partial^2 w_x}{\partial y^2} \right) + d_2^2 \left(\frac{\partial^2 u_x}{\partial x^2} - 2 \frac{\partial^2 u_y}{\partial x \partial y} - \frac{\partial^2 u_x}{\partial y^2} \right) \\ \frac{\partial w_y}{\partial t} &= d_1^2 \left(\frac{\partial^2 w_y}{\partial x^2} + \frac{\partial^2 w_y}{\partial y^2} \right) + d_2^2 \left(\frac{\partial^2 u_y}{\partial x^2} + 2 \frac{\partial^2 u_x}{\partial x \partial y} - \frac{\partial^2 u_y}{\partial y^2} \right) \end{aligned} \quad (6)$$

where

$$c_1 = \sqrt{\frac{L+2M}{\rho}}, c_2 = \sqrt{\frac{M}{\rho}}, c_3 = \sqrt{\frac{R}{\rho}}, d_1 = \sqrt{\frac{K_1}{\kappa}}, d_2 = \sqrt{\frac{R}{\kappa}}$$

Note that constants c_1, c_2 and c_3 have the meaning of elastic wave speeds, while d_1 and d_2 do not represent wave speed, and d_1^2 and d_2^2 are diffusive coefficients in physical meaning.

A decagonal quasicrystal with a crack is shown in Fig.1. It is a rectangular specimen with a central crack of length $2a(t)$ subjected to a dynamic or static tensile stress at its edges ED and FC, in which $a(t)$ represents the crack length being a function of time, and for dynamic initiation of crack growth, the crack is stable, so $a(t) = a_0 = \text{constant}$, for fast crack propagation, $a(t)$ varies with time. At first we consider dynamic initiation of crack growth, then study crack fast propagation. Due to the symmetry of the specimen only the upper right quarter is considered.

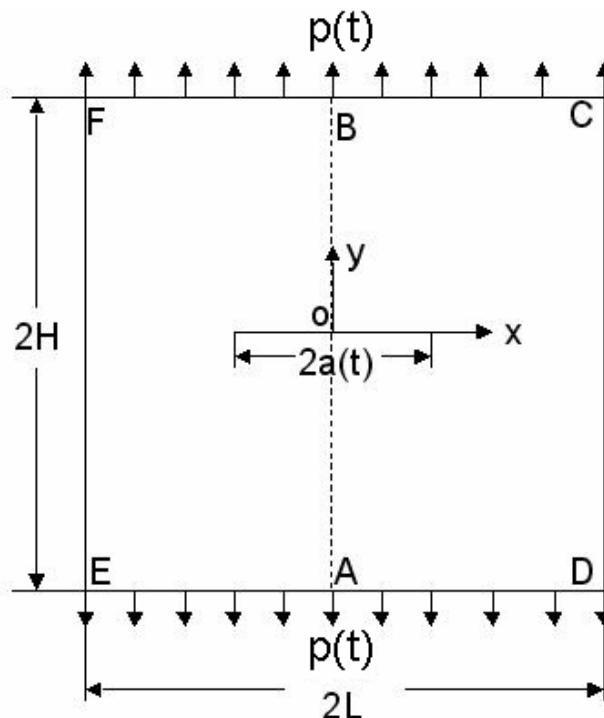


Fig. 1. The specimen with a central crack

Referring to the upper right part and considering a fix grips case, the following boundary conditions should be satisfied:

$$\begin{aligned}
 u_x = 0, \sigma_{yx} = 0, w_x = 0, H_{yx} = 0 & \quad \text{on } x = 0 \text{ for } 0 \leq y \leq H \\
 \sigma_{xx} = 0, \sigma_{yx} = 0, H_{xx} = 0, H_{yx} = 0 & \quad \text{on } x = L \text{ for } 0 \leq y \leq H \\
 \sigma_{yy} = p(t), \sigma_{xy} = 0, H_{yy} = 0, H_{xy} = 0 & \quad \text{on } y = H \text{ for } 0 \leq x \leq L \\
 \sigma_{yy} = 0, \sigma_{xy} = 0, H_{yy} = 0, H_{xy} = 0 & \quad \text{on } y = 0 \text{ for } 0 \leq x \leq a(t) \\
 u_y = 0, \sigma_{xy} = 0, w_y = 0, H_{xy} = 0 & \quad \text{on } y = 0 \text{ for } a(t) \leq x \leq L
 \end{aligned} \tag{7}$$

in which $p(t) = p_0 f(t)$ is a dynamic load if $f(t)$ varies with time, otherwise it is a static load (i.e., if $f(t) = \text{const}$), and $p_0 = \text{const}$ with the stress dimension.

The initial conditions are

$$\begin{aligned} u_x(x, y, t)|_{t=0} &= 0 & u_y(x, y, t)|_{t=0} &= 0 \\ w_x(x, y, t)|_{t=0} &= 0 & w_y(x, y, t)|_{t=0} &= 0 \\ \frac{\partial u_x(x, y, t)}{\partial t}|_{t=0} &= 0 & \frac{\partial u_y(x, y, t)}{\partial t}|_{t=0} &= 0 \end{aligned} \quad (8)$$

For implementation of finite difference all field variables in governing equations (6) and boundary-initial conditions (7), (8) must be expressed by displacements and their derivatives. This can be done through the constitutive equations (2). The detail of the finite difference scheme is omitted here but can be referred to Fan [1].

For the related parameters in this section, the experimentally determined mass density for decagonal Al-Ni-Co quasicrystal $\rho = 4.186 \times 10^{-3} \text{ g} \cdot \text{mm}^{-3}$ is used and phonon elastic moduli are $C_{11} = 2.3433 \times 10^{12} \text{ dyn/cm}^2$, $C_{12} = 0.5741 \times 10^{12} \text{ dyn/cm}^2$ ($10^{10} \text{ dyn/cm}^2 = \text{GPa}$) which are obtained by resonant ultrasound spectroscopy, refer to Chernikov et al [6], we have also chosen phason elastic constants $K_1 = 1.22 \times 10^{12} \text{ dyn/cm}^2$ and $K_2 = 0.24 \times 10^{12} \text{ dyn/cm}^2$ ($10^{10} \text{ dyn/cm}^2 = \text{GPa}$) estimated by Monto-Carlo simulation given by Jeong and Steinhardt [7] and $\Gamma_w = 1/\kappa = 4.8 \times 10^{-19} \text{ m}^3 \cdot \text{s/kg} = 4.8 \times 10^{-10} \text{ cm}^3 \cdot \mu\text{s/g}$ which measured by de Boussieu and collected by Walz in his master thesis [8]. The coupling constant R has been measured for some special cases recently, see Chapter 6 and Chapter 9 of monograph written by Fan [1] respectively. In computation we take $R/M = 0.01$ for coupling case corresponding to quasicrystals, and $R/M = 0$ for decoupled case which corresponds to crystals.

2.2 Examination on the physical model

In order to verify the correctness of the suggested model and the numerical simulation, we first explore the specimen without a crack. We know that there are the fundamental solutions characterizing time variation natures based on wave propagation of phonon field and on motion of diffusion of phason, respectively according to mathematical physics

$$\begin{cases} u \sim e^{i\omega(t-x/c)} \\ w \sim \frac{1}{\sqrt{t-t_0}} e^{-(x-x_0)^2/\Gamma_w(t-t_0)} \end{cases} \quad (9)$$

where ω is a frequency and c a speed of the wave, t the time and t_0 a special value of t , x the distance, x_0 a special value of x , and Γ_w the kinetic coefficient of phason defined previously.

Comparison results are shown in Fig.2 (a-c), in which the solid line represents the numerical solution of quasicrystals and the dotted line represents fundamental solution given by formulas (9). From Fig. 2(a) and (b) we can see that both displacement components of phonon field are in excellent agreement to the fundamental solutions of mathematical physics. However, there are some differences because the phonon field is influenced by phason field

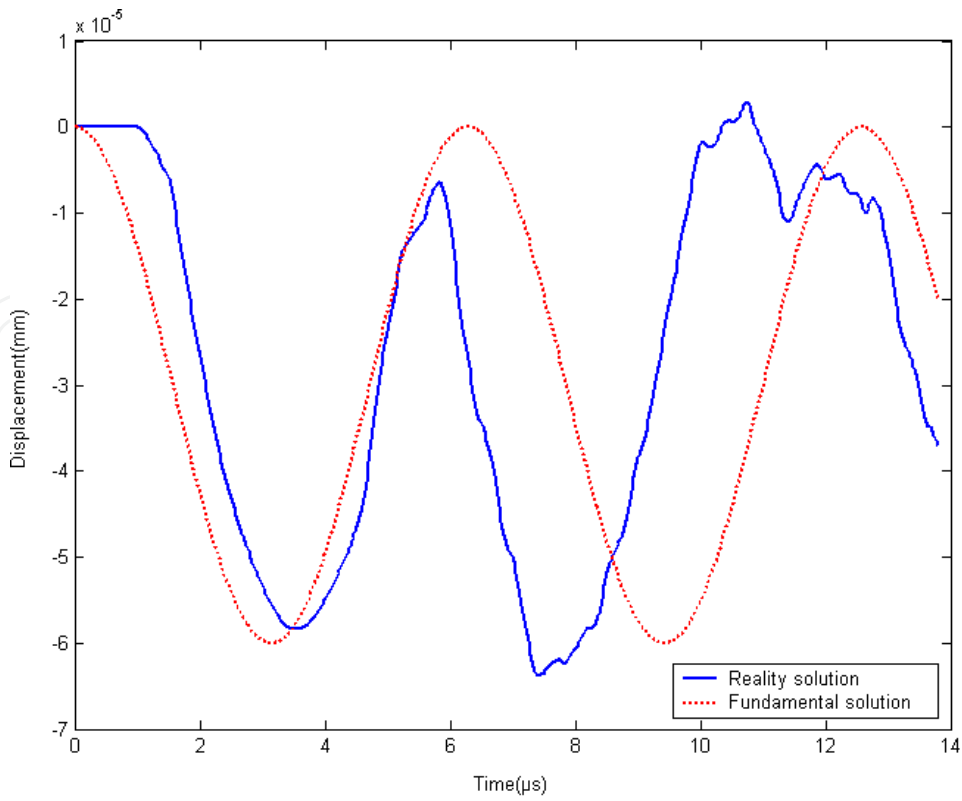


Fig. 2. (a) Displacement component of phonon field u_x versus time

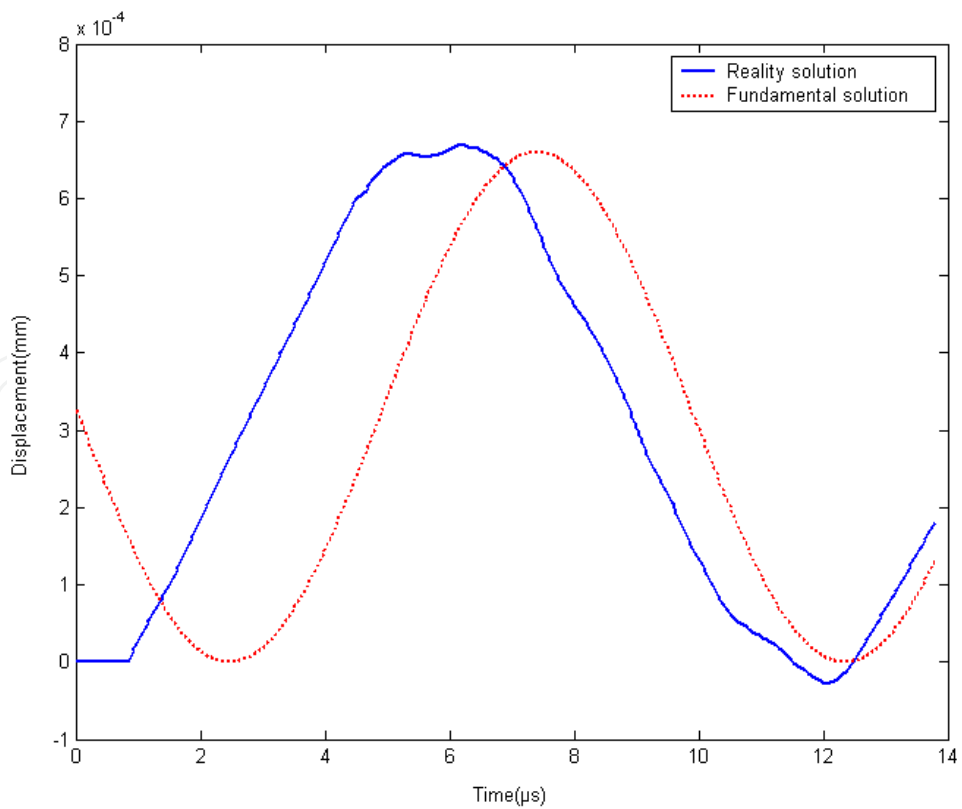


Fig. 2. (b) Displacement component of phonon field u_y versus time

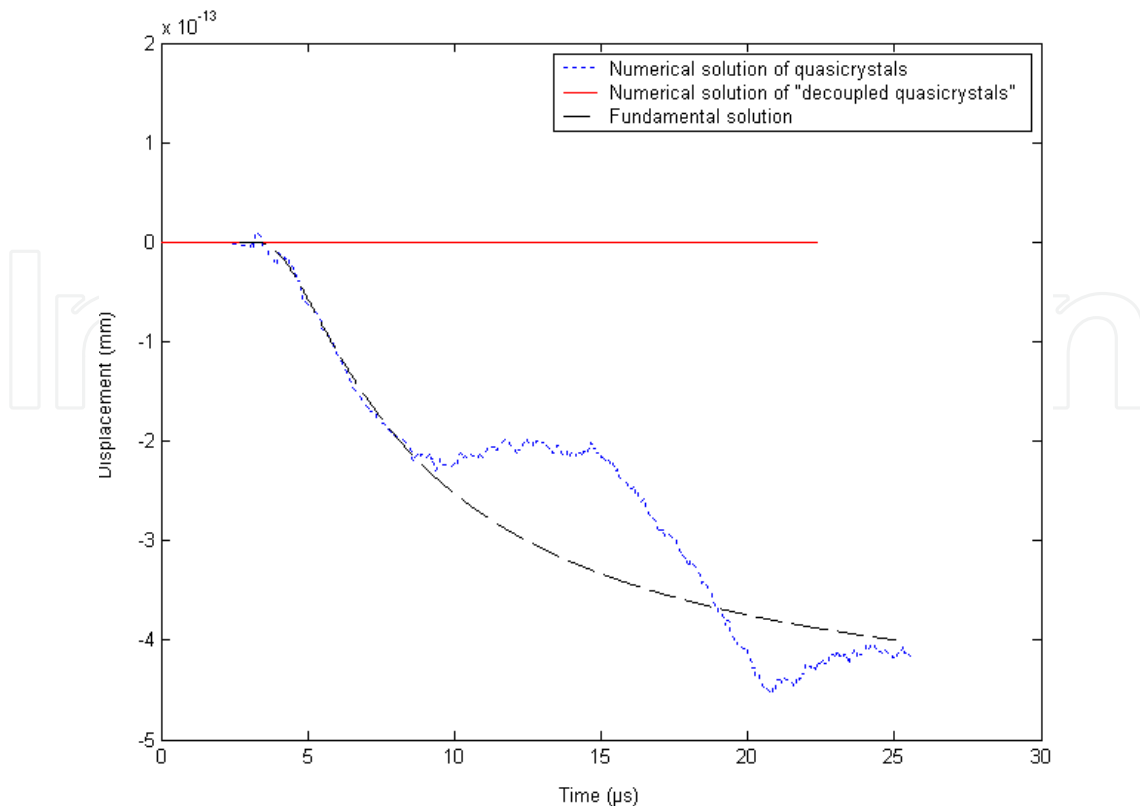


Fig. 2. (c) Displacement component of phason field w_x versus time

and the phonon-phason coupling effect. From Fig. 2(c), in the phason field we find that the phason mode presents diffusive nature in the overall tendency, but because of influence of the phonon and phonon-phason coupling, it can also have some characters of fluctuation. So the model describes the dynamic behaviour of phonon field and phason field in deed. This also shows the mathematical modeling of the present work is valid.

2.3 Testing the scheme and the computer program

2.3.1 Stability of the scheme

The stability of the scheme is the core problem of finite difference method which depends upon the choice of parameter $\alpha = c_1\tau/h$, which is the ratio between time step and space step substantively. The choice is related to the ratio c_1/c_2 , i.e., the ratio between speeds of elastic longitudinal and transverse waves of the phonon field. To determine the upper bound for the ration to guarantee the stability, according to our computational practice and considering the experiences of computations for conventional materials, we choose $\alpha = 0.8$ in all cases and results are stable.

2.3.2 Accuracy test

The stability is only a necessary condition for successful computation. We must check the accuracy of the numerical solution. This can be realized through some comparison with some well-known classical solutions (analytic as well as numerical solutions) of conventional fracture mechanics. For this purpose the material constants in the computation are chosen as $c_1 = 7.34 \text{ mm}/\mu\text{s}$, $c_2 = 3.92 \text{ mm}/\mu\text{s}$ and $\rho = 5 \times 10^3 \text{ kg}/\text{m}^3$, $p_0 = 1 \text{ MPa}$ which

are the same with those given in classical references for conventional fracture dynamics, discussed in Fan's monograph [1] in detail. At first the comparison to the classical exact analytic solution is carried out, in this case we put $w_x = w_y = 0$ (i.e., $K_1 = K_2 = R = 0$) for the numerical solution. The comparison has been done with the key physical quantity—dynamic stress intensity factor, which is defined by

$$K_I(t) = \lim_{x \rightarrow a_0^+} \sqrt{\pi(x - a_0)} \sigma_{yy}(x, 0, t) \quad (10)$$

The normalized dynamic stress intensity factor can be denoted as $K_I(t) / K_I^{static}$, in which K_I^{static} is the corresponding static stress intensity factor, whose value here is taken as $\sqrt{\pi a_0} p_0$. For the dynamic initiation of crack growth in classical fracture dynamics there is the only exact analytic solution—the Maue's solution (refer to Fan's monograph [1]), but the configuration of whose specimen is quite different from that of our specimen. Maue studied a semi-infinite crack in an infinite body, and subjected to a Heaviside impact loading at the crack surface. While our specimen is a finite size rectangular plate with a central crack, and the applied stress is at the external boundary of the specimen. Generally the Maue's model cannot describe the interaction between wave and external boundary. However, consider a very short time interval, i.e., during the period between the stress wave from the external boundary arriving at the crack tip (this time is denoted by t_1) and before the reflecting by external boundary stress wave emanating from the crack tip in the finite size specimen (the time is marked as t_2). During this special very short time interval our specimen can be seen as an "infinite specimen". The comparison given by Fig. 3 shows the numerical results are in excellent agreement with those of Maue's solution within the short interval in which the solution is valid.

Our solution corresponding to case of $w_x = w_y = 0$ is also compared with numerical solutions of conventional crystals, e.g. Murti's solution and Chen's solutions (refer to Fan [1] and Zhu and Fan [9] for the detail), which are also shown in Fig. 3, it is evident, our solution presents very high precise.

2.3.3 Influence of mesh size (space step)

The mesh size or the space step of the algorithm can influence the computational accuracy too. To check the accuracy of the algorithm we take different space steps shown in Table 1, which indicates if $h = a_0 / 40$ the accuracy is good enough. The check is carried out through static solution, because the static crack problem in infinite body of decagonal quasicrystals has exact solution given in Chapter 8 of monograph given by Fan [1], and the normalized static intensity factor is equal to unit. In the static case, there is no wave propagation effect, $L / a_0 \geq 3, H / a_0 \geq 3$ the effect of boundary to solution is very weak, and for our present specimen $L / a_0 \geq 4, H / a_0 \geq 8$, which may be seen as an infinite specimen, so the normalized static stress intensity factor is approximately but with highly precise equal to unit. The table shows that the algorithm is with a quite highly accuracy when $h = a_0 / 40$.

2.4 Results of dynamic initiation of crack growth

The dynamic crack problem presents two "phases" in the process: the dynamic initiation of crack growth and fast crack propagation. In the phase of dynamic initiation of crack growth, the length of the crack is constant, assuming $a(t) = a_0$. The specimen with stationary crack

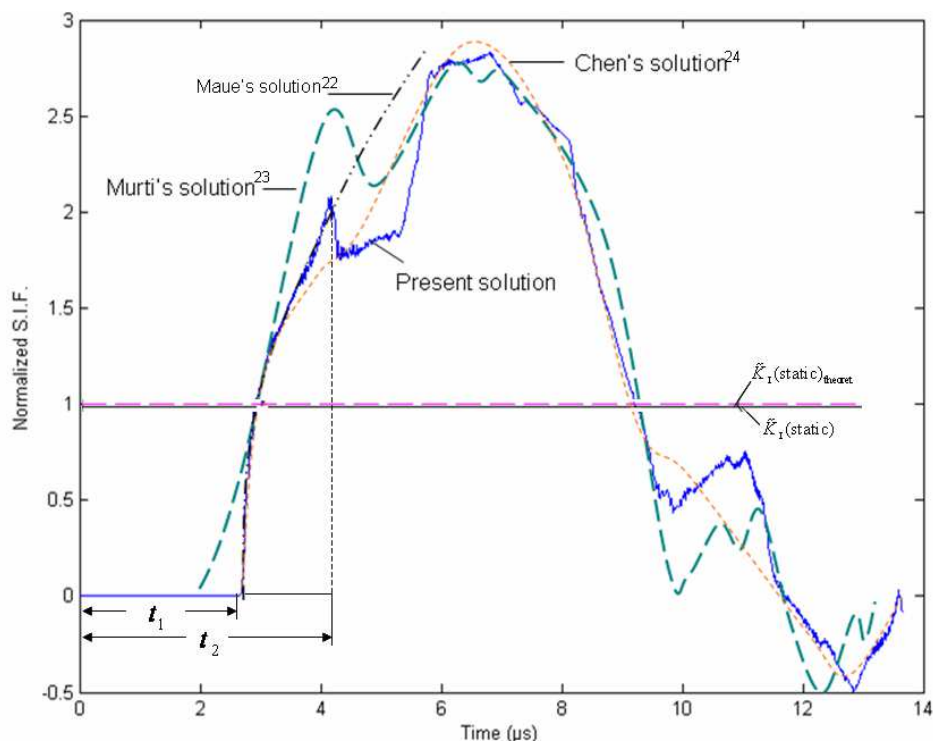


Fig. 3. Comparison of the present solution with analytic solution and other numerical solution for conventional structural materials given by other authors

H	$a_0/10$	$a_0/15$	$a_0/20$	$a_0/30$	$a_0/40$
K	0.9259	0.94829	0.9229	0.97723	0.99516
Errors	7.410%	5.171%	3.771%	2.277%	0.484%

Table 1. The normalized static S.I.F. of quasicrystals for different space steps

that are subjected to a rapidly varying applied load $p(t) = p_0 f(t)$, where p_0 is a constant with stress dimension and $f(t)$ is taken as the Heaviside function. It is well known the coupling effect between phonon and phason is very important, which reveals the distinctive physical properties including mechanical properties, and makes quasicrystals distinguish the periodic crystals. So studying the coupling effect is significant.

The dynamic stress intensity factor $K_I(t)$ for quasicrystals has the same definition given by equation (10), whose numerical results are plotted in Fig. 4, where the normalized dynamics stress intensity factor $K_I(t)/\sqrt{\pi a_0 p_0}$ is used. There are two curves in the Fig. 4, one represents quasicrystal, i.e., $R/M = 0.01$, the other describes periodic crystals corresponding to $R/M = 0$, the two curves of the Fig. 4 are apparently different, though they are similar to some extends. Because of the phonon-phason coupling effect, the mechanical properties of the quasicrystals are obviously different from the classical crystals. Thus, the coupling effect plays an important role.

In Fig. 4, t_0 represents the time that the wave from the external boundary propagates to the crack surface, in which $t_0 = 2.6735 \mu\text{s}$. So the velocity of the wave propagation is $v_0 = H/t_0 = 7.4807 \text{ km/s}$, which is just equal to the longitudinal wave speed $c_1 = \sqrt{(L+2M)/\rho}$. This indicates that for the complex system of wave propagation-motion of diffusion coupling, the phonon wave propagation presents dominating role.

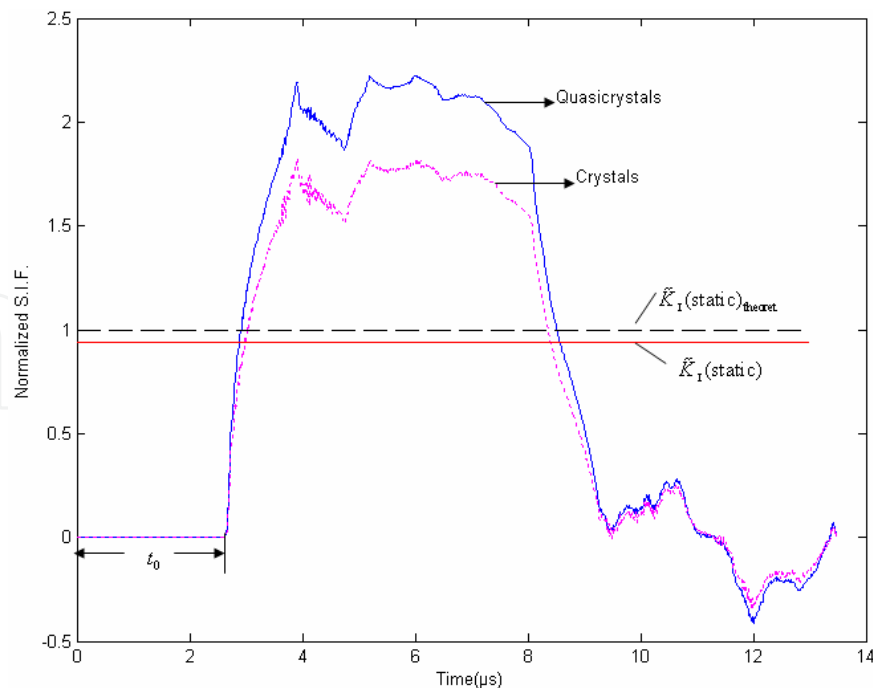


Fig. 4. Normalized dynamics stress intensity factor (DSIF) versus time

There are some oscillations of values of the stress intensity factor in the figure. These oscillations characterize the reflection and diffraction between waves coming from the crack surface and the specimen boundary surfaces. The oscillations are influenced by the material constants and specimen geometry including the shape and size very much.

3. Elasto-/hydro-dynamics and applications to fracture dynamics of three-dimensional icosahedral quasicrystals

3.1 Basic equations, boundary and initial conditions

There are over 50% icosahedral quasicrystals among observed the quasicrystals to date, this shows this kind of systems in the material presents the most importance. Within icosahedral quasicrystals, the icosahedral Al-Pd-Mn quasicrystals are concerned in particular by researchers, for which especially a rich set of experimental data for elastic constants accumulated so far, this is useful to the computational practice. So we focus on the elasto-hydrodynamics of icosahedral Al-Pd-Mn quasicrystals here. From the previous section we have known there are lack of measured data for phason elastic constants, the computation has to take some data which are obtained by Monte Carlo simulation, this makes some undetermined factors for computational results for decagonal quasicrystals. This shows the discussion on icosahedral quasicrystals is more necessary, and the formalism and numerical results are presented in the following.

If considering only the plane problem, especially for the crack problems, there are much of similarities with those discussed in the previous section. We present herein only the part that are different.

For the plane problem, i.e.,

$$\frac{\partial(\)}{\partial z} = 0 \quad (11)$$

The linearized elasto-hydrodynamics of icosahedral quasicrystals have non-zero displacements u_z, w_z apart from u_x, u_y, w_x, w_y , so in the strain tensors

$$\varepsilon_{ij} = \frac{1}{2} \left(\frac{\partial u_i}{\partial x_j} + \frac{\partial u_j}{\partial x_i} \right) \quad w_{ij} = \frac{\partial w_i}{\partial x_j}$$

it increases some non-zero components compared with those in two-dimensional quasicrystals. In connecting with this, in the stress tensors, the non-zero components increase too relatively to two-dimensional ones. With these reasons, the stress-strain relation presents different nature with that of decagonal quasicrystals though the generalized Hooke's law has the same form with that in one- and two-dimensional quasicrystals, i.e.,

$$\sigma_{ij} = C_{ijkl} \varepsilon_{kl} + R_{ijkl} w_{kl} \quad H_{ij} = R_{klij} \varepsilon_{kl} + K_{ijkl} w_{kl}$$

In particular the elastic constants are quite different from those discussed in the previous sections, in which the phonon elastic constants can be expressed such as

$$C_{ijkl} = \lambda \delta_{ij} \delta_{kl} + \mu (\delta_{ik} \delta_{jl} + \delta_{il} \delta_{jk}) \quad (12)$$

and the phason elastic constant matrix [K] and phason-phason coupling elastic one [R] are defined by the formulas of Fan's monograph [1], which are not listed here again.

Substituting these non-zero stress components into the equations of motion

$$\rho \frac{\partial^2 u_i}{\partial t^2} = \frac{\partial \sigma_{ij}}{\partial x_j}, \quad \kappa \frac{\partial w_i}{\partial t} = \frac{\partial H_{ij}}{\partial x_j} \quad (13)$$

and through the generalized Hooke's law and strain-displacement relation we obtain the final dynamic equations as follows

$$\begin{aligned} \frac{\partial^2 u_x}{\partial t^2} + \theta \frac{\partial u_x}{\partial t} &= c_1^2 \frac{\partial^2 u_x}{\partial x^2} + (c_1^2 - c_2^2) \frac{\partial^2 u_y}{\partial x \partial y} + c_2^2 \frac{\partial^2 u_x}{\partial y^2} + c_3^2 \left(\frac{\partial^2 w_x}{\partial x^2} + 2 \frac{\partial^2 w_y}{\partial x \partial y} - \frac{\partial^2 w_x}{\partial y^2} \right) \\ \frac{\partial^2 u_y}{\partial t^2} + \theta \frac{\partial u_y}{\partial t} &= c_2^2 \frac{\partial^2 u_y}{\partial x^2} + (c_1^2 - c_2^2) \frac{\partial^2 u_x}{\partial x \partial y} + c_1^2 \frac{\partial^2 u_y}{\partial y^2} + c_3^2 \left(\frac{\partial^2 w_y}{\partial x^2} - 2 \frac{\partial^2 w_x}{\partial x \partial y} - \frac{\partial^2 w_y}{\partial y^2} \right) \\ \frac{\partial^2 u_z}{\partial t^2} + \theta \frac{\partial u_z}{\partial t} &= c_2^2 \left(\frac{\partial^2}{\partial x^2} + \frac{\partial^2}{\partial y^2} \right) u_z + c_3^2 \left(\frac{\partial^2 w_x}{\partial x^2} - \frac{\partial^2 w_x}{\partial y^2} - 2 \frac{\partial^2 w_y}{\partial x \partial y} + \frac{\partial^2 w_z}{\partial x^2} + \frac{\partial^2 w_z}{\partial y^2} \right) \\ \frac{\partial w_x}{\partial t} + \theta w_x &= d_1 \left(\frac{\partial^2}{\partial x^2} + \frac{\partial^2}{\partial y^2} \right) w_x + d_2 \left(\frac{\partial^2}{\partial x^2} - \frac{\partial^2}{\partial y^2} \right) w_z + d_3 \left(\frac{\partial^2 u_x}{\partial x^2} - 2 \frac{\partial^2 u_y}{\partial x \partial y} - \frac{\partial^2 u_x}{\partial y^2} + \frac{\partial^2 u_z}{\partial x^2} - \frac{\partial^2 u_z}{\partial y^2} \right) \\ \frac{\partial w_y}{\partial t} + \theta w_y &= d_1 \left(\frac{\partial^2}{\partial x^2} + \frac{\partial^2}{\partial y^2} \right) w_y - d_2 \frac{\partial^2 w_z}{\partial x \partial y} + d_3 \left(\frac{\partial^2 u_y}{\partial x^2} + 2 \frac{\partial^2 u_x}{\partial x \partial y} - \frac{\partial^2 u_y}{\partial y^2} - 2 \frac{\partial^2 u_z}{\partial x \partial y} \right) \\ \frac{\partial w_z}{\partial t} + \theta w_z &= (d_1 - d_2) \left(\frac{\partial^2}{\partial x^2} + \frac{\partial^2}{\partial y^2} \right) w_z + d_2 \left(\frac{\partial^2 w_x}{\partial x^2} - \frac{\partial^2 w_x}{\partial y^2} - 2 \frac{\partial^2 w_y}{\partial x \partial y} \right) + d_3 \left(\frac{\partial^2}{\partial x^2} + \frac{\partial^2}{\partial y^2} \right) u_z \end{aligned} \quad (14)$$

in which

$$c_1 = \sqrt{\frac{\lambda + 2\mu}{\rho}}, c_2 = \sqrt{\frac{\mu}{\rho}}, c_3 = \sqrt{\frac{R}{\rho}}, d_1 = \frac{K_1}{\kappa}, d_2 = \frac{K_2}{\kappa}, d_3 = \frac{R}{\kappa} \quad (15)$$

note that constants c_1, c_2 and c_3 have the meaning of elastic wave speeds, while d_1, d_2 and d_3 do not represent wave speed, but are diffusive coefficients and parameter θ may be understood as a manmade damping coefficient as in the previous section.

Consider an icosahedral quasicrystal specimen with a Griffith crack shown in Fig. 1, all parameters of geometry and loading are the same with those given in the previous, but in the boundary conditions there are some different points, which are given as below

$$\begin{aligned} u_x = 0, \sigma_{yx} = 0, \sigma_{zx} = 0, w_x = 0, H_{yx} = 0, H_{zx} = 0 & \quad \text{on } x = 0 \text{ for } 0 \leq y \leq H \\ \sigma_{xx} = 0, \sigma_{yx} = 0, \sigma_{zx} = 0, H_{xx} = 0, H_{yx} = 0, H_{zx} = 0 & \quad \text{on } x = L \text{ for } 0 \leq y \leq H \\ \sigma_{yy} = p(t), \sigma_{xy} = 0, \sigma_{zy} = 0, H_{yy} = 0, H_{xy} = 0, H_{zy} = 0 & \quad \text{on } y = H \text{ for } 0 \leq x \leq L \\ \sigma_{yy} = 0, \sigma_{xy} = 0, \sigma_{zy} = 0, H_{yy} = 0, H_{xy} = 0, H_{zy} = 0 & \quad \text{on } y = 0 \text{ for } 0 \leq x \leq a(t) \\ u_y = 0, \sigma_{xy} = 0, \sigma_{zy} = 0, w_y = 0, H_{xy} = 0, H_{zy} = 0 & \quad \text{on } y = 0 \text{ for } a(t) < x \leq L \end{aligned} \quad (16)$$

The initial conditions are

$$\begin{aligned} u_x(x, y, t)|_{t=0} = 0 \quad u_y(x, y, t)|_{t=0} = 0 \quad u_z(x, y, t)|_{t=0} = 0 \\ w_x(x, y, t)|_{t=0} = 0 \quad w_y(x, y, t)|_{t=0} = 0 \quad w_z(x, y, t)|_{t=0} = 0 \\ \frac{\partial u_x(x, y, t)}{\partial t}|_{t=0} = 0 \quad \frac{\partial u_y(x, y, t)}{\partial t}|_{t=0} = 0 \quad \frac{\partial u_z(x, y, t)}{\partial t}|_{t=0} = 0 \end{aligned} \quad (17)$$

3.2 Some results

We now concentrate on investigating the phonon and phason fields in the icosahedral Al-Pd-Mn quasicrystal, in which we take $\rho = 5.1 \text{ g/cm}^3$ and $\lambda = 74.2 \text{ GPa}, \mu = 70.4 \text{ GPa}$ of the phonon elastic moduli, for phason ones $K_1 = 72 \text{ MPa}, K_2 = -37 \text{ MPa}$ and the constant relevant to diffusion coefficient of phason is $\Gamma_w = 1/\kappa = 4.8 \times 10^{-19} \text{ m}^3 \cdot \text{s/kg} = 4.8 \times 10^{-10} \text{ cm}^3 \cdot \mu\text{s/g}$. On the phonon-phason coupling constant, there is no measured result for icosahedral quasicrystals so far, we take $R/\mu = 0.01$ for quasicrystals, and $R/\mu = 0$ for "decoupled quasicrystals" or crystals.

The problem is solved by the finite difference method, the principle, scheme and algorithm are illustrated as those in the previous section, and shall not be repeated here. The testing for the physical model, scheme, algorithm and computer program are similar to those given in Section 2. The numerical results for dynamic initiation of crack growth problem, the phonon and phason displacements are shown in Fig. 5.

The dynamic stress intensity factor $K_I(t)$ is defined by

$$K_I(t) = \lim_{x \rightarrow a_0^+} \sqrt{\pi(x - a_0)} \sigma_{yy}(x, 0, t)$$

and the normalized dynamics stress intensity factor (D.S.I.F.) $\tilde{K}_I(t) = K_I(t) / \sqrt{\pi a_0 p_0}$ is used, the results are illustrated in Fig. 6, in which the comparison with those of crystals are shown, one can see the effects of phason and phonon-phason coupling are evident very much.

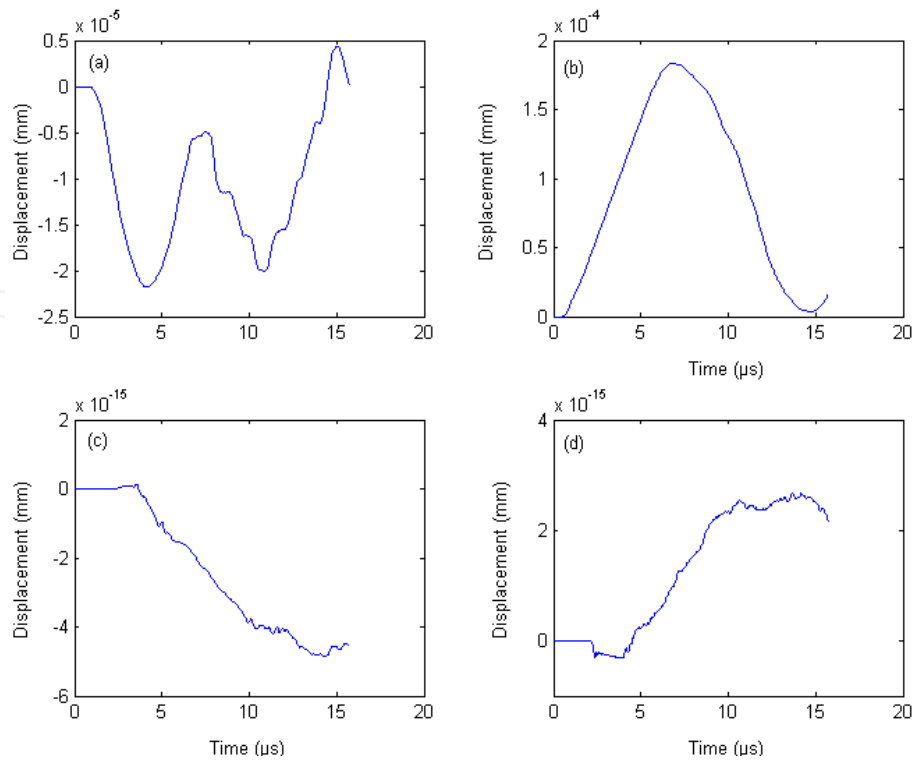


Fig. 5. Displacement components of quasicrystals versus time.
 (a) displacement component u_x ; (b) displacement component u_y ;
 (c) displacement component w_x ; (d) displacement component w_y

For the fast crack propagation problem the primary results are listed only the dynamic stress intensity factor versus time as below

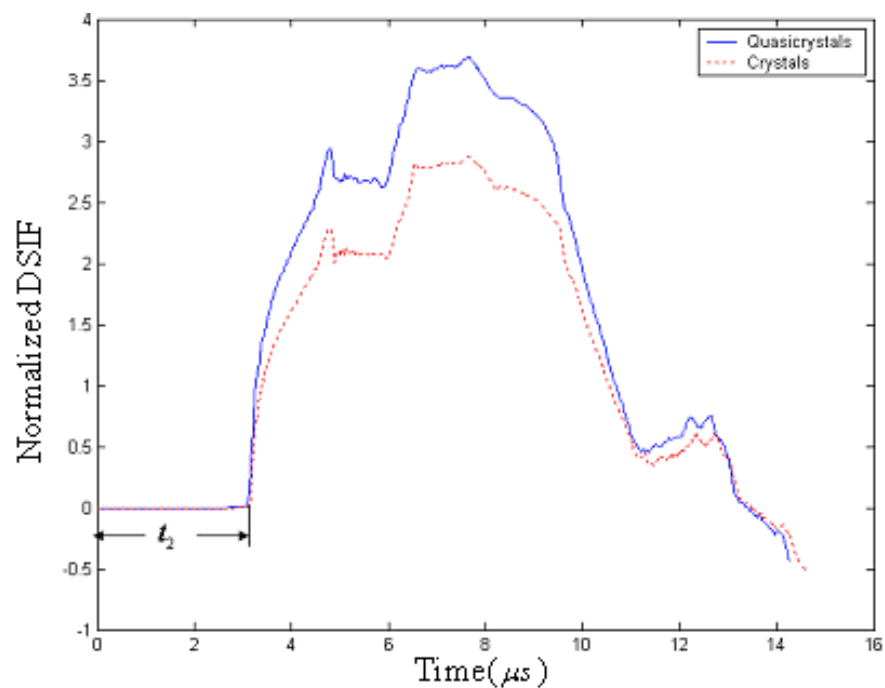


Fig. 6. Normalized dynamic stress intensity factor of central crack specimen under impact loading versus time

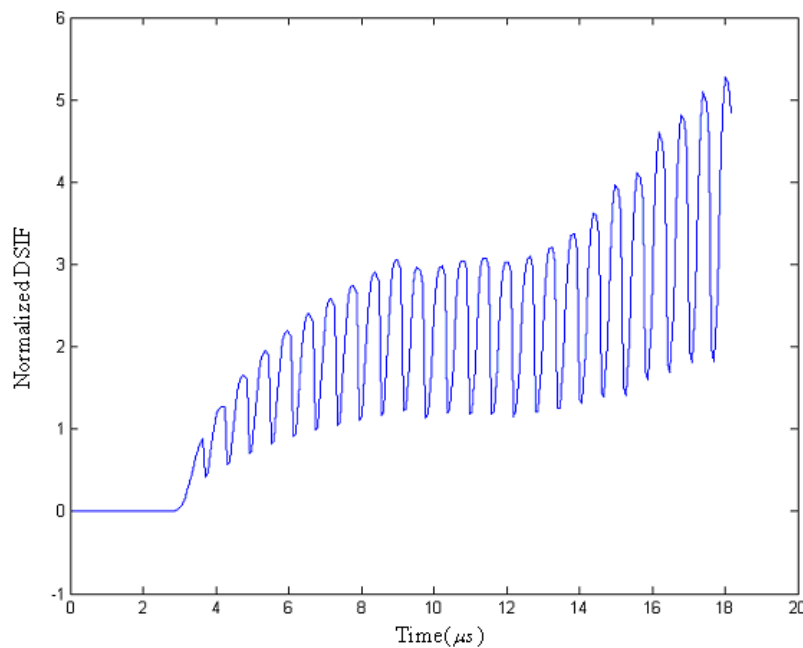


Fig. 7. Normalized stress intensity factor of propagating crack with constant crack speed versus time.

Details of this work can be given by Fan and co-workers [1], [10].

4. Conclusion and discussion

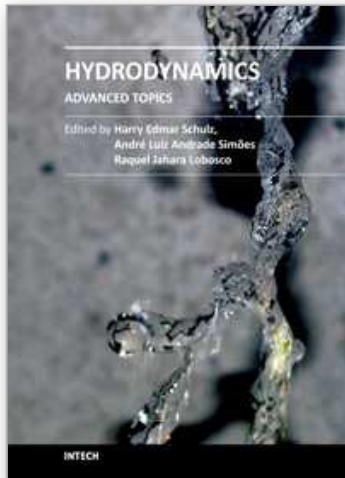
In Sections 1 through 3 a new model on dynamic response of quasicrystals based on argument of Lubensky et al is formulated. This model is regarded as an elasto-hydrodynamics model for the material, or as a collaborating model of wave propagation and diffusion. This model is more complex than pure wave propagation model for conventional crystals, the analytic solution is very difficult to obtain, except a few simple examples introduced in Fan's monograph [1]. Numerical procedure based on finite difference algorithm is developed. Computed results confirm the validity of wave propagation behaviour of phonon field, and behaviour of diffusion of phason field. The interaction between phonons and phasons are also recorded.

The finite difference formalism is applied to analyze dynamic initiation of crack growth and crack fast propagation for two-dimensional decagonal Al-Ni-Co and three-dimensional icosahedral Al-Pd-Mn quasicrystals, the displacement and stress fields around the tip of stationary and propagating cracks are revealed, the stress present singularity with order $r^{-1/2}$, in which r denotes the distance measured from the crack tip. For the fast crack propagation, which is a nonlinear problem—moving boundary problem, one must provide additional condition for determining solution. For this purpose we give a criterion for checking crack propagation/crack arrest based on the critical stress criterion. Application of this additional condition for determining solution has helped us to achieve the numerical simulation of the moving boundary value problem and revealed crack length-time evolution. However, more important and difficult problems are left open for further study. Up to now the arguments on the physical meaning of phason variables based on hydrodynamics within different research groups have not been ended yet, see e.g. Coddens [11], which may be solved by further experimental and theoretical investigations.

5. References

- [1] Fan T Y, 2010, *Mathematical Theory of Elasticity of Quasicrystals and Its Applications*, Beijing:Science Press/Heidelberg:Springer-Verlag.
- [2] Lubensky T C , Ramaswamy S and Joner J, 1985, Hydrodynamics of icosahedral quasicrystals, *Phys. Rev. B*, 32(11), 7444.
- [3] Socolar J E S, Lubensky T C and Steinhardt P J, 1986, Phonons, phasons and dislocations in quasicrystals, *Phys. Rev. B*, 34(5), 3345.
- [4] Rochal S B and Lorman V L, 2002 , Minimal model of the phonon-phason dynamics on icosahedral quasicrystals and its application for the problem of internal friction in the i-AIPdMn alloys, *Phys. Rev. B*, 66 (14), 144204.
- [5] Fan T Y , Wang X F, Li W et al., 2009, Elasto-hydrodynamics of quasicrystals, *Phil. Mag.*, 89(6),501.
- [6] Chernikov M A, Ott H R, Bianchi A et al., 1998, Elastic moduli of a single quasicrystal of decagonal Al-Ni-Co: evidence for transverse elastic isotropy, *Phys. Rev. Lett.* 80(2), 321-324.
- [7] H. C. Jeong and P. J. Steinhardt, 1993, Finite-temperature elasticity phase transition in decagonal quasicrystals , *Phys. Rev. B* 48(13), 9394.
- [8] Walz C, 2003, *Zur Hydrodynamik in Quasikristallen*, Diplomarbeit, Universitaet Stuttgart.
- [9] Zhu A Y and Fan T Y, 2008, Dynamic crack propagation in a decagonal Al-Ni-Co quasicrystal , *J. Phys.: Condens. Matter*, 20(29), 295217.
- [10] Wang X F, Fan T Y and Zhu A Y, 2009, Dynamic behaviour of the icosahedral Al-Pd-Mn quasicrystal with a Griffith crack, *Chin Phys B*, 18 (2), 709.(or referring to Zhu A Y: Study on analytic and numerical solutions in elasticity of three-dimensional quasicrystals and elastodynamics of two- and three-dimensional quasicrystals, Dissertation, Beijing Institute of Technology, 2009)
- [11] Coddens G, 2006, On the problem of the relation between phason elasticity and phason dynamics in quasicrystals, *Eur. Phys. J. B*, 54(1), 37.

IntechOpen



Hydrodynamics - Advanced Topics

Edited by Prof. Harry Schulz

ISBN 978-953-307-596-9

Hard cover, 442 pages

Publisher InTech

Published online 22, December, 2011

Published in print edition December, 2011

The phenomena related to the flow of fluids are generally complex, and difficult to quantify. New approaches - considering points of view still not explored - may introduce useful tools in the study of Hydrodynamics and the related transport phenomena. The details of the flows and the properties of the fluids must be considered on a very small scale perspective. Consequently, new concepts and tools are generated to better describe the fluids and their properties. This volume presents conclusions about advanced topics of calculated and observed flows. It contains eighteen chapters, organized in five sections: 1) Mathematical Models in Fluid Mechanics, 2) Biological Applications and Biohydrodynamics, 3) Detailed Experimental Analyses of Fluids and Flows, 4) Radiation-, Electro-, Magnetohydrodynamics, and Magnetorheology, 5) Special Topics on Simulations and Experimental Data. These chapters present new points of view about methods and tools used in Hydrodynamics.

How to reference

In order to correctly reference this scholarly work, feel free to copy and paste the following:

Tian You Fan and Zhi Yi Tang (2011). Elasto-Hydrodynamics of Quasicrystals and Its Applications, Hydrodynamics - Advanced Topics, Prof. Harry Schulz (Ed.), ISBN: 978-953-307-596-9, InTech, Available from: <http://www.intechopen.com/books/hydrodynamics-advanced-topics/elasto-hydrodynamics-of-quasicrystals-and-its-applications>

INTECH
open science | open minds

InTech Europe

University Campus STeP Ri
Slavka Krautzeka 83/A
51000 Rijeka, Croatia
Phone: +385 (51) 770 447
Fax: +385 (51) 686 166
www.intechopen.com

InTech China

Unit 405, Office Block, Hotel Equatorial Shanghai
No.65, Yan An Road (West), Shanghai, 200040, China
中国上海市延安西路65号上海国际贵都大饭店办公楼405单元
Phone: +86-21-62489820
Fax: +86-21-62489821

© 2011 The Author(s). Licensee IntechOpen. This is an open access article distributed under the terms of the [Creative Commons Attribution 3.0 License](#), which permits unrestricted use, distribution, and reproduction in any medium, provided the original work is properly cited.

IntechOpen

IntechOpen